Journal of Biomechanics 44 (2011) 1621–1625

Contents lists available at ScienceDirect

Journal of Biomechanics

journal homepage: www.elsevier.com/locate/jbiomech
www.JBiomech.com

Short communication

A two-parameter model of the effective elastic tensor for cortical bone

Quentin Grimal [a,b,*], Guillermo Rus [c], William J. Parnell [d], Pascal Laugier [a,b]

[a] UPMC Univ Paris 06, UMR 7623, LIP, F-75005 Paris, France
[b] CNRS, UMR 7623, Laboratoire d'Imagerie Paramétrique, F-75005 Paris, France
[c] Department of Structural Mechanics, University of Granada, 18071 Granada, Spain
[d] School of Mathematics, Alan Turing Building, University of Manchester, Manchester, M13 9PL, UK

ARTICLE INFO

Article history:
Accepted 4 March 2011

Keywords:
Cortical bone
Model
Homogenization
Elasticity
Anisotropy

ABSTRACT

Multiscale models of cortical bone elasticity require a large number of parameters to describe the organization and composition of the tissue. We hypothesize that the macro-scale anisotropic elastic properties of different bones can be modeled retaining only two variable parameters, and setting the others to universal values identical for all bones. Cortical bone is regarded as a two-phase composite material: a dense mineralized matrix (ultrastructure) and a soft phase (pores). The ultrastructure is assumed to be a homogeneous and transversely isotropic tissue whose elastic properties in different directions are mutually dependent and can be scaled with a single parameter driving the overall rigidity. This parameter is taken to be the volume fraction of mineral f_{ha}. The pore network is modeled as an ensemble of water-filled cylinders and described only by the porosity p. The effective macroscopic elasticity tensor $C_{ij}(f_{ha},p)$ is calculated with a multiscale micromechanics approach starting from existing models. The modeled stiffness coefficients compare favorably to four literature datasets which were chosen because they provide the full stiffness tensors of groups of human samples. Since the physical counterparts of f_{ha} and p were unknown for the datasets, their values which allow the best fit of experimental tensors by the modeled ones were determined by optimization. Optimum values of f_{ha} and p are found to be unique and realistic. These results suggest that a two-parameter model may be sufficient to model the elasticity of different samples of human femora and tibiae. Such a model would in particular be useful in large-scale parametric studies of bone mechanical response.

1. Introduction

Macroscopic effective elastic coefficients of cortical bone can be predicted by multiscale models given relative amounts of the elementary constituents and assumed organizational patterns. Multiscale models generally require a large number of parameters to describe the tissue at each scale. For instance, authors have considered variations of the volume fraction of vascular porosity (Hellmich et al., 2004b; Baron et al., 2007; Parnell and Grimal, 2009); volume fraction of pores at different scales (Sevostianov and Kachanov, 2000); relative area of osteonal, interstitial tissue and resorption cavities (Dong and Guo, 2006); organization patterns of the mineral (Crolet et al., 2005); patterns of osteonal lamellae (Crolet et al., 1993; Aoubiza et al., 1996). In addition, the models usually consider different volume fractions of elementary constituents. Models with a large number of parameters are difficult to validate since several combinations of the parameter values may result in similar effective elasticity values to be compared to experiments.

This communication investigates a simple multiscale model of mature Haversian bone elasticity. We hypothesize that macro-scale anisotropic properties of different bones can be recovered to some extent by a model using only two parameters: porosity and mineral content. Elastic constants of the phases and organizational patterns are fixed for all bones. The model lends itself to a comprehensive analysis of the role of each parameter and can be critically assessed with experimental data.

2. Method

Cortical bone is regarded as a two-phase composite with a transversely isotropic (TI) mineralized matrix (ultrastructure) pervaded by cylindrical pores (vascular porosity). The 'mineral foam matrix with collagen inclusions' micromechanical model (Hellmich et al., 2004a) is used for the ultrastructure because of its limited number of variables. It is based on two idealizations: (1) at a length scale of 100 nm, hydroxyapatite crystals and ultrastructural water with non-collagenous organic material constitutes a mineral foam; (2) at a length scale of 5 to 10 microns, collagen fibers are embedded into the mineral foam. The stiffness

* Corresponding author. Laboratoire d'Imagerie Paramétrique, CNRS, UMR 7623, 15, Rue de l'Ecole de Medecine, 75006 Paris, France. Tel.: +33144414972; fax: +33146335673.
E-mail address: quentin.grimal@upmc.fr (Q. Grimal).

0021-9290/$ - see front matter © 2011 Elsevier Ltd. All rights reserved.
doi:10.1016/j.jbiomech.2011.03.006

of the elementary constituents (collagen, mineral and water) are fixed to some assumed universal values and their volume fractions denoted f_{ha}, f_{col}, and f_w (respectively) are the only 'variable' parameters of the ultrastructure model. Since $f_{ha}+f_{col}+f_w=1$ the model in fact has two independent parameters. Raum et al. (2006) proposed an empirical law (Eq. (10) of that paper) based on experimental data by Broz et al. (1995) which relates f_{col}/f_w to f_{ha}. With the latter relationship, the number of parameters of the ultrastructure model is reduced to one. Here, we choose f_{ha}, as the independent parameter. This model was first used by Grimal et al. (2008) to estimate millimeter scale effective properties of cortical bone, which were in agreement with experimental data.

The volume fraction of the vascular porosity is denoted p. The effective properties of the representative volume element consisting of the TI matrix (ultrastructure) pervaded by cylindrical inclusions with a circular cross-section and volume fraction p (cylinder axes are aligned with the axis of rotational symmetry of the TI matrix) were calculated with the Mori–Tanaka scheme (Zaoui, 2002). The bulk modulus of pores was set to 2.2 or 10^{-5} GPa for undrained and drained pores, respectively, and the shear modulus in both cases was 10^{-9} GPa. For the analysis of the model response, the range of parameter values was taken somewhat larger than the documented range of mineral content (Hellmich et al., 2004a) and porosity (Bousson et al., 2004): $f_{ha}\in[0.3\text{–}0.5]$ and $p\in[0\text{–}20\%]$.

For an orthotropic material with principal directions aligned with the frame $(\mathbf{x}_1,\mathbf{x}_2,\mathbf{x}_3)$, C_{ii} $(i=1\cdots3)$ denote the longitudinal stiffnesses, C_{ii} $(i=4\cdots6)$ denote the shear moduli and only three non-diagonal terms are different from zero: C_{12}, C_{13}, C_{23}. With the direction of the long bone axis taken parallel to $\mathbf{x}_3$, the material is TI, which means $C_{11}=C_{22}$, $C_{44}=C_{55}$, $C_{13}=C_{23}$, and $C_{66}=(C_{11}-C_{12})/2$. Finally, macro-scale effective elastic coefficients depend on two parameters; we write $C_{ij}=C_{ij}(f_{ha},p)$. A program to compute the model response is provided as supplementary website material.

The literature was reviewed in order to define datasets of macroscopic measured stiffness constants C^e_{ij} appropriate to assess the model. These fulfill the conditions: (1) measurements of cortical bone samples obtained from mature human subjects; (2) full set of C^e_{ij} available to describe the material in an orthotropic or TI framework. We found four datasets referred to as EXP1-4 (Table 1); C^e_{ij} are reported in Table 3 with the corresponding modeled C_{ij} for convenience.

Because there is no available dataset to directly compare C_{ij} and C^e_{ij} for known values of f_{ha} and p, we tested the model according to its ability to fit each experimental stiffness tensor. A cost function (CF) is defined as

$$H_0(f_{ha},p,\mathbf{C}^e)=\sqrt{\hat{\sum_{i,j=1}^{6}}\left(\frac{C^e_{ij}-C_{ij}(f_{ha},p)}{C^e_{ij}}\right)^2}, \tag{1}$$

where $\hat{\sum}$ denotes summation over the upper triangular part of the stiffness matrix. The CF minimizes the error over all the elements of the stiffness tensor. Other CFs with different weights for each coefficient were tested but they could not improve the fits. The optimal set of parameters was obtained for each dataset by solving a minimization problem that consists in finding (f_{ha},p) such that $H_0(f_{ha},p,\mathbf{C}^e)$ is a minimum.

The comparison between modeled and experimental elastic properties was performed for stiffness coefficients and engineering moduli: Young modulus E_3 and shear modulus G_{12}. The stiffness tensor was rotated successively around axes $\mathbf{x}_1$, $\mathbf{x}_2$, and $\mathbf{x}_3$ between 0 and $\pi/2$. E_3 and G_{12} were retrieved from the inverted rotated tensors which yields moduli at different angles with respect to the material symmetry axes $(\mathbf{x}_1,\mathbf{x}_2,\mathbf{x}_3)$.

Table 1
Experimental data sets ($\mathbf{C}^e$) taken from references Ashman et al. (1984), Yoon and Katz (1976), Rho (1996) and Taylor et al. (2002) for EXP1-4, respectively. All values correspond to averages on several bone specimen obtained from one or several subjects as indicated, except EXP2. Samples from EXP2 were dried (drained pores) prior to measurements, samples in EXP1, 2, and 3 were measured in moist state (undrained pores).

	EXP1	EXP2	EXP3	EXP4
Specimen (human)	5 femurs	1 femur	8 tibiae	1 femur
Number of samples (material volume)	60	2	96	10
Pore status	moist	dry	moist	moist
Anisotropic framework	orthotropic	TI	orthotropic	orthotropic

3. Results

Stiffness coefficients vary between 20% and 70% in the tested parameter range (Figs. 1 and 2). They decrease with increasing p and increase with increasing f_{ha}. Compared to other coefficients, C_{33} depends greatly on f_{ha} but weakly on p; C_{11} is more influenced by variations in p than f_{ha}. Shear coefficients C_{44} and C_{66} are greatly influenced by both parameters. Non-diagonal coefficients C_{12} and C_{13} have relatively small variations.

For the four datasets, the CF had a unique minimum in the parameter plane. Determined values of p and f_{ha} fall within the range of physiological values (Table 2). A smaller value of the CF is obtained for EXP2 and the worst fit for EXP3. We observed that taking the wrong pore status in the model (i.e. undrained pores while the experimental data was obtained for drained pores, or the opposite) leads to unphysical values of p and f_{ha} (data not shown). Setting mechanical properties of pores in between the properties corresponding to drained and undrained also lead to poor results. This is an indication that the influence of the hydratation state of the pores was modeled correctly. Macroscopic C_{ij} (Table 3) calculated with the optimum parameters (Table 2) yield the best fit to experimental values.

The angular dependence of Young and shear moduli are plotted for the best (EXP2, Fig. 3) and the worst (EXP3, Fig. 4) fits. The discrepancies between experimental and modeled moduli for the two other datasets are bounded by the discrepancies observed in these two cases. The model provides an excellent estimation of the angular variation of the moduli for EXP2. For EXP3, the agreement is better for Young modulus than shear modulus; for all angles, model estimation is within less than 20% of the experimental data and much less for a wide range of angles.

4. Discussion

With two parameters, the model can fit the 5–9 independently measured stiffness constants of each dataset with relatively good

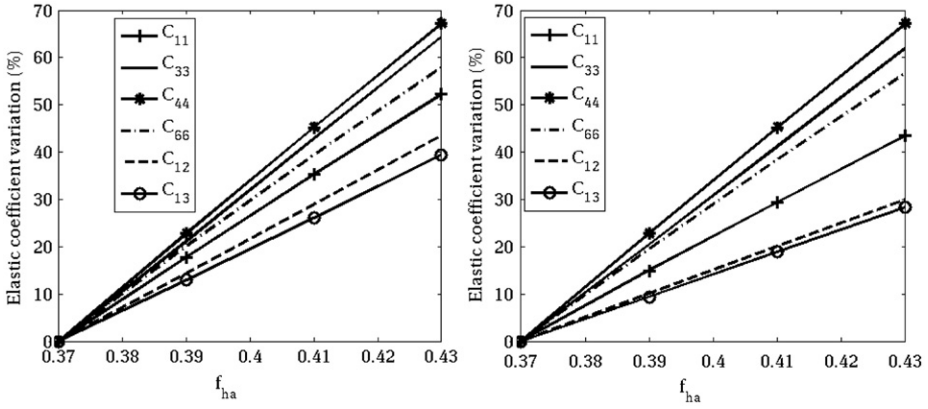

Fig. 1. Sensitivity of effective macroscopic stiffness to parameter f_{ha} for 1% porosity (left) and 30% porosity (right). Values on the y-axis represent the percentage of variation for a reference value at $f_{ha}=0.37$.

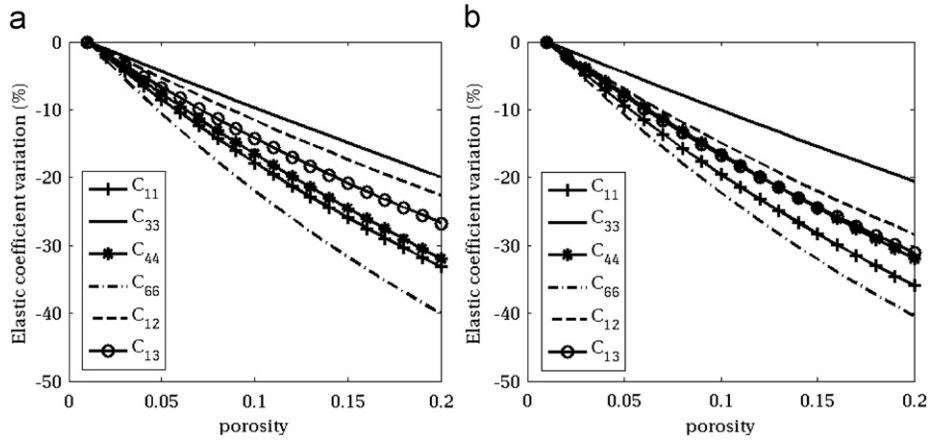

Fig. 2. Sensitivity of effective macroscopic stiffness to porosity for $f_{ha}=0.37$ (left) and $f_{ha}=0.44$ (right). Values on the y-axis represent the percentage of variation for a reference value at 1% porosity.

Table 2
Determined values of model parameters which minimize the cost function H_0 (Eq. 1).

	EXP1	EXP2	EXP3	EXP4
p	11.3 %	7.1 %	13.3 %	2.5 %
f_{ha}	0.396	0.423	0.398	0.399
CF	0.4578	0.0925	0.7449	0.5750

Table 3
Coefficients of the stiffness tensor (GPa): experimental values C_{ij}^e (first line); model values C_{ij} (second line). Dependent coefficients in TI framework are indicated.

	C_{11}	C_{22}	C_{33}	C_{44}	C_{55}	C_{66}	C_{12}	C_{13}	C_{23}
EXP1	18.0	20.2	27.6	6.2	5.6	4.5	10.0	10.1	10.7
	18.7	$=C_{11}$	26.4	6.3	$=C_{44}$	5.5	7.7	8.2	$=C_{13}$
EXP2	23.4	$=C_{11}$	32.5	8.7	$=C_{44}$	7.2	9.1	9.1	$=C_{13}$
	23.2	$=C_{11}$	33.5	8.5	$=C_{44}$	7.4	8.5	9.4	$=C_{13}$
EXP3	19.5	20.2	31.0	5.7	5.2	4.1	11.5	12.7	12.7
	18.2	$=C_{11}$	26.3	6.2	$=C_{44}$	5.3	7.6	8.0	$=C_{13}$
EXP4	24.9	26.2	33.3	7.1	6.6	5.7	11.0	13.6	14.0
	23.4	$=C_{11}$	30.1	7.8	$=C_{44}$	7.2	9.0	9.8	$=C_{13}$

accuracy. This is despite the many idealizations necessary to derive the model, in particular those leading to the ultrastructure model: the osteonal structure and small pores (osteocyte lacunae, canaliculli) are not modeled. The results suggest that a simple ultrastructure model may be sufficient to model the mineralized matrix anisotropy. It is likely that similar or better agreement could be obtained with other micromechanical models than the one used here (Akkus, 2005; Yoon and Cowin, 2008; Deuerling et al., 2009; Reisinger et al., 2010).

Except EXP2, all datasets are averages of stiffness values for several samples, either from different donors or different anatomical locations. Accordingly we cannot judge the ability of the model to predict the inter-sample stiffness variability. We have in fact tested the ability of the model to account for the 'average' anisotropic macroscopic properties of different sample groups (Table 1). An important limitation of the datasets is that the actual mineral content and porosity have not been assessed, which prevents the validation of the values of the determined parameters (f_{ha} and p). The construction of datasets including stiffness tensor measurements, porosity and mineral content for the same samples is necessary to further validate the model.

An original methodology was developed to evaluate the ability of a model to fit experimental data. By defining a CF and using an optimization algorithm, it was possible to perform a critical test of the model. The variation of the CF with parameter values should be smooth enough for a 'good' model. If many local minima exist, the optimization problem is ill-posed, i.e. the optimization algorithm could converge to various parameter values. Here, the CF has a convex behavior so that the minimum is unique.

The parameters f_{ha} and p are supposed to represent the actual mineral content and porosity. It is noteworthy that the determined values are realistic. f_{ha} should be interpreted as the *apparent* mineral content of the mineralized matrix rather that the actual mineral content: it drives the overall matrix stiffness and may account for other factors than mineral content which also have an impact on stiffness (osteon type, crystal properties, small pores, etc.). The range of variation of the average mineral content (in a millimeter volume) of bone is still a matter of dispute, but it is established that the latter does not vary greatly (Akkus et al., 2003; Bergot et al., 2009). Typical values of mineral content are 1.1 g/cc (Boivin and Meunier, 2002) which, given a mass density of biological hydroxyapatite of 3 g/cc (Lees, 1987), leads to a volume fraction of 0.37. This value is close to the determined f_{ha} which are around 0.4 for all datasets. Determined mineral content of EXP2 is slightly higher which may be due to the fact that the samples were dried before measurements, which is a known cause of stiffening (Wolfram et al., 2010). Determined values of p are likely to be somewhat influenced by the determined values of f_{ha} because they are coupled through the CF. While p should reflect the actual vascular porosity, it should also be interpreted with care.

The results suggest the feasibility of modeling cortical bone macroscopic elasticity with only two parameters. This is in contrast to most of the existing multiscale models. It was well known that porosity is an important parameter (see, e.g. Dong and Guo, 2004). The results presented here establish that the anisotropic and heterogeneous elastic properties of the mineralized matrix can be accounted for by an ultrastructure model with a single parameter (in this study, f_{ha}) which scales the matrix rigidity. The proposed model is too simple to account for minute changes of tissue composition and organization. With a single parameter governing matrix anisotropy the model is not appropriate to model variations in elastic anisotropy that are independent of tissue density (Espinoza Orias et al., 2009). The model should be useful to build subject-specific bone models at the organ scale. State-of-the-art subject-specific organ-scale models use isotropic (Helgason et al., 2008; Duchemin et al., 2008) or anisotropic (Hellmich et al., 2008) elastic constants derived from X-ray attenuation data. Our model can be used to simulate the variations of bone anisotropic elasticity with the mineral content and porosity and used as input in stochastic simulations (Macocco et al., 2006; Laz et al., 2007; Santos et al., 2009). Another application is the regularization of multiparameter cortical bone

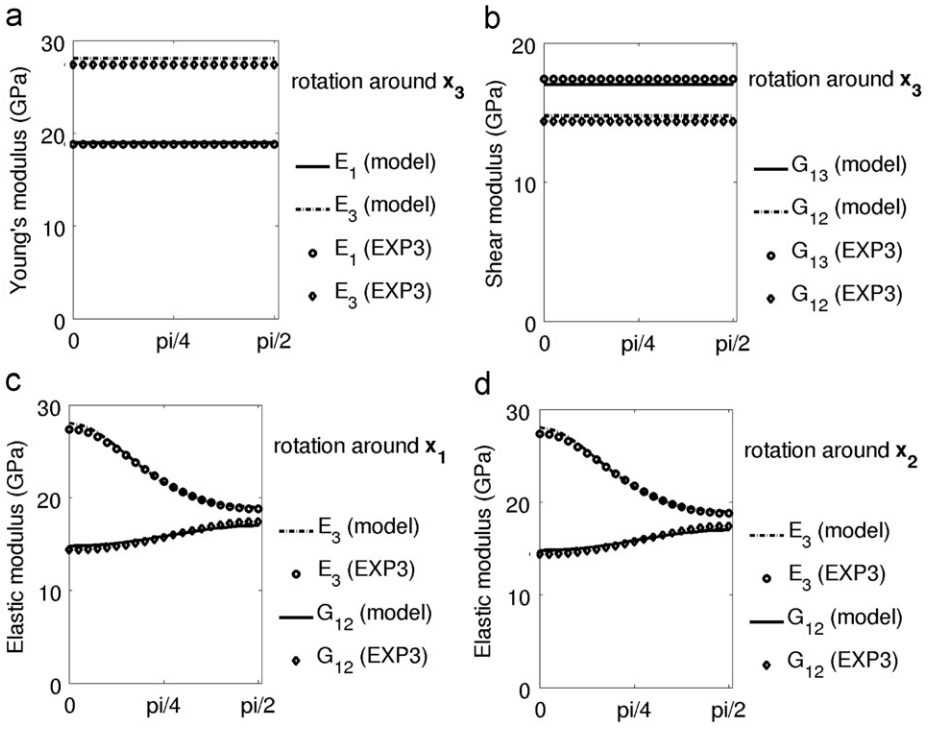

Fig. 3. Angular dependence of Young and shear moduli for EXP2 (best fit).

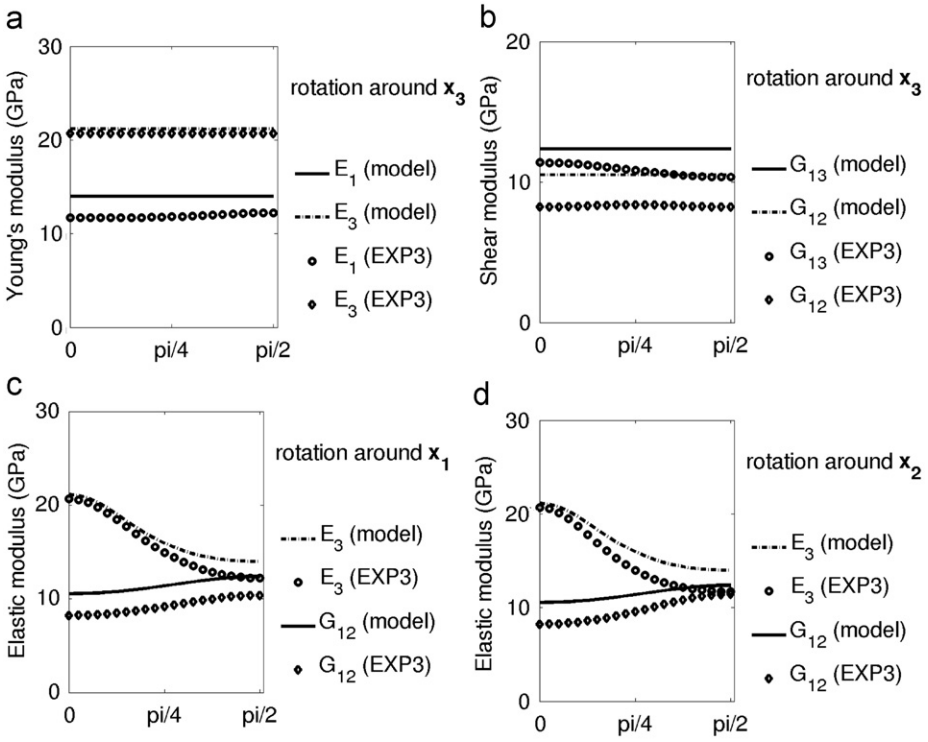

Fig. 4. Angular dependence of Young and shear moduli for EXP3 (worst fit).

characterization problems using data retrieved *in vivo* with ultrasound (Talmant et al., 2009).

Conflict of interest statement

No conflict of interest.

Acknowledgments

G. Rus wishes to acknowledge the Ministerio de Ciencia e Innovación for a research grant in program 'Jose Castillejo' 2008. W.J. Parnell is grateful to EPSRC for funding via his 'Overseas Travel Grant' (EP/G064512/1) and 'First Grant' (EP/H010114/1). W.J. Parnell and Q. Grimal would like to point out

that the work was also conducted in the framework of GDR CNRS 2501.

Appendix A. Supplementary data

Supplementary data associated with this article can be found in the online version at doi:10.1016/j.radphyschem.2011.02.020.

References

Akkus, O., 2005. Elastic deformation of mineralized collagen fibrils: an equivalent inclusion based composite model. J. Biomech. Eng.—Trans. ASME 127 (3), 383–390.

Akkus, O., Polyakova-Akkus, A., Adar, F., Schaffler, M.B., 2003. Aging of microstructural compartments in human compact bone. J. Bone. Miner. Res. 18 (6), 1012–1019.

Aoubiza, B., Crolet, J.M., Meunier, A., 1996. On the mechanical characterization of compact bone structure using the homogenization theory. J. Biomech. 29 (12), 1539–1547.

Ashman, R.B., Cowin, S.C., Van Buskirk, W.C, Rice, J.C., 1984. A continuous wave technique for the measurement of the elastic properties of cortical bone. J. Biomech. 17 (5), 349–361.

Baron, C., Talmant, M., Laugier, P., 2007. Effect of porosity on effective diagonal stiffness coefficients (Cii) and elastic anisotropy of cortical bone at 1 MHz: a finite-difference time domain study. J. Acoust. Soc. Am. 122 (3), 1810–1817.

Bergot, C., Wu, Y., Jolivet, E., Zhou, L.Q., Laredo, J.D., Bousson, V., 2009. The degree and distribution of cortical bone mineralization in the human femoral shaft change with age and sex in a microradiographic study. Bone 45 (3), 435–442.

Boivin, G., Meunier, P.J., 2002. The degree of mineralization of bone tissue measured by computerized quantitative contact microradiography. Calcif. Tissue Int. 70 (6), 503–511.

Bousson, V., Peyrin, F., Bergot, C., Hausard, M., Sautet, A., Laredo, J.D., 2004. Cortical bone in the human femoral neck: three-dimensional appearance and porosity using synchrotron radiation. J. Bone Miner. Res. 19 (5), 794–801.

Broz, J.J., Simske, S.J., Greenberg, A.R., 1995. Material and compositional properties of selectively demineralized cortical bone. J. Biomech. 28 (11), 1357–1368.

Crolet, J.M., Aoubiza, B., Meunier, A., 1993. Compact bone: numerical simulation of mechanical characteristics. J. Biomech. 26 (6), 677–687.

Crolet, J.M., Racila, M., Mahraoui, R., Meunier, A., 2005. A new numerical concept for modeling hydroxyapatite in human cortical bone. Comput. Meth. Biomech. Biomed. Eng. 8 (2), 139–143.

Deuerling, J.M., Yue, W., Espinoza Orias, A.A., Roeder, R.K., 2009. Specimen-specific multi-scale model for the anisotropic elastic constants of human cortical bone. J. Biomech. 42 (13), 2061–2067.

Dong, X.N., Guo, X.E., 2004. The dependence of transversely isotropic elasticity of human femoral cortical bone on porosity. J. Biomech. 37 (8), 1281–1287.

Dong, X.N., Guo, X.E., 2006. Prediction of cortical bone elastic constants by a two-level micromechanical model using a generalized self-consistent method. J. Biomech. Eng.—Trans. ASME 128 (3), 309–316.

Duchemin, L., Mitton, D., Jolivet, E., Bousson, V., Laredo, J.D., Skalli, W., 2008. An anatomical subject-specific FE-model for hip fracture load prediction. Comput. Meth. Biomech. Biomed. Eng. 11 (2), 105–111.

Espinoza Orias, A.A., Deuerling, J.M., Landrigan, M.D., Renaud, J.E., Roeder, R.K., 2009. Anatomic variation in the elastic anisotropy of cortical bone tissue in the human femur. J. Mech. Behav. Biomed. Mater. 2 (3), 255–263.

Grimal, Q., Raum, K., Gerisch, A., Laugier, P., 2008. Derivation of the mesoscopic elasticity tensor of cortical bone from quantitative impedance images at the micron scale. Comput. Meth. Biomech. Biomed. Eng. 11 (2), 147–157.

Helgason, B., Perilli, E., Schileo, E., Taddei, F., Brynjolfsson, S., Viceconti, M., 2008. Mathematical relationships between bone density and mechanical properties: a literature review. Clin. Biomech. 23 (2), 135–146.

Hellmich, C., Barthelemy, J., Dormieux, L., 2004a. Mineral-collagen interactions in elasticity of bone ultrastructure - a continuum micromechanics approach. Eur. J. Mech. A—Solids 23 (5), 783–810.

Hellmich, C., Ulm, F.J., Dormieux, L., 2004b. Can the diverse elastic properties of trabecular and cortical bone be attributed to only a few tissue-independent phase properties and their interactions? Arguments from a multiscale approach. Biomech. Model. Mechanobiol. 2 (4), 219–238.

Hellmich, C., Kober, C., Erdmann, B., 2008. Micromechanics-based conversion of CT data into anisotropic elasticity tensors, applied to FE simulations of a mandible. Ann. Biomed. Eng. 36 (1), 219–222.

Laz, P.J., Stowe, J.Q., Baldwin, M.A., Petrella, A.J., Rullkoetter, P.J., 2007. Incorporating uncertainty in mechanical properties for finite element-based evaluation of bone mechanics. J. Biomech. 40 (13), 2831–2836.

Lees, S., 1987. Considerations regarding the structure of the mammalian mineralized osteoid from viewpoint of the generalized packing model. Connect. Tissue Res. 16 (4), 281–303.

Macocco, K., Grimal, Q., Naili, S., Soize, C., 2006. Elastoacoustic model with uncertain mechanical properties for ultrasonic wave velocity prediction: application to cortical bone evaluation. J. Acoust. Soc. Am. 119 (2), 729–740.

Parnell, W.J., Grimal, Q., 2009. The influence of mesoscale porosity on cortical bone anisotropy. Investigations via asymptotic homogenization. J. R. Soc. Interface 6 (30), 97–109.

Raum, K., Cleveland, R.O., Peyrin, F., Laugier, P., 2006. Derivation of elastic stiffness from site-matched mineral density and acoustic impedance maps. Phys. Med. Biol. 51 (3), 747–758.

Reisinger, A.G., Pahr, D.H., Zysset, P.K., 2010. Sensitivity analysis and parametric study of elastic properties of an unidirectional mineralized bone fibril-array using mean field methods. Biomech. Model. Mechanobiol. 9 (5), 499–510.

Rho, J.Y., 1996. An ultrasonic method for measuring the elastic properties of human tibial cortical and cancellous bone. Ultrasonics 34 (8), 777–783.

Santos, V.J., Bustamante, C.D., Valero-Cuevas, F.J., 2009. Improving the fitness of high-dimensional biomechanical models via data-driven stochastic exploration. IEEE Trans. Biomed. Eng. 56 (3), 552–564.

Sevostianov, I., Kachanov, M., 2000. Impact of the porous microstructure on the overall elastic properties of the osteonal cortical bone. J. Biomech. 33 (7), 881–888.

Talmant, M., Kolta, S., Roux, C., Haguenauer, D., Vedel, I., Cassou, B., Bossy, E., Laugier, P., 2009. In vivo performance evaluation of bi-directional ultrasonic axial transmission for cortical bone assessment. Ultrasound Med. Biol. 35 (6), 912–919.

Taylor, W.R., Roland, E., Ploeg, H., Hertig, D., Klabunde, R., Warner, M.D., Hobatho, M.C., Rakotomanana, L., Clift, S.E., 2002. Determination of orthotropic bone elastic constants using FEA and modal analysis. J. Biomech. 35 (6), 767–773.

Wolfram, U., Wilke, H.J., Zysset, P.K., 2010. Valid micro finite element models of vertebral trabecular bone can be obtained using tissue properties measured with nanoindentation under wet conditions. J. Biomech. 43 (9), 1731–1737.

Yoon, H.S., Katz, J.L., 1976. Ultrasonic wave propagation in human cortical bone—II. Measurements of elastic properties and microhardness. J. Biomech. 9 (7), 459–464.

Yoon, Y.J., Cowin, S.C., 2008. The estimated elastic constants for a single bone osteonal lamella. Biomech. Model. Mechanobiol. 7 (1), 1–11.

Zaoui, A., 2002. Continuum micromechanics: survey. J. Eng. Mech.—ASCE 128 (8), 808–816 Conference on Mechanics and Materials, San Diego, CA, Jun 26–29, 2001.